PD-Vol. 64-7, Engineering Systems Design and Analysis
Volume 7
ASME 1994

INSTABILITY THRESHOLD AND STABILITY BOUNDARIES OF ROTOR-BEARING SYSTEMS

W. J. Chen
Centrifugal Compressor Division
Ingersoll-Rand Company
Mayfield, Kentucky

ABSTRACT

A direct numerical method for the determination of instability threshold and stability boundaries of flexible rotor-bearing systems is presented. The stability boundary of an operating parameter is established by examining the variation in the real part of eigenvalue as a function of the operating parameter. This procedure can also be used to improve the system stability by considering the design variables as operating parameters. The finite element method is utilized in the formulation of system equations of motion. The numerical algorithm is based on the nonlinear optimization techniques. Two examples are presented to illustrate the feasibility, desirability and the ability of the proposed algorithm. A simple journal bearing system is used for the parametric study. An industrial high speed compressor is employed to demonstrate the ability of this algorithm to deal with the practical applications. The stability boundaries calculated from this algorithm are in agreement with the experimental results.

NOMENCLATURE

C	damping
$\mathbf{C}$	damping matrix
C_B	bearing radial clearance
C_L	lobe radial clearance
D	bearing diameter
F	force
f	objective function
$\mathbf{G}$	gyroscopic matrix
L	bearing length
K	stiffness
$\mathbf{K}$	stiffness matrix
$\mathbf{K}^*$	state space matrix defined by equation (9)
m	preload
$\mathbf{M}$	mass/inertia matrix
$\mathbf{M}^*$	state space matrix defined by equation (9)
N_S	rotor speed, rps
n	degrees of freedom
$\mathbf{p}$	operating parameter vector
$\mathbf{Q}$	force vector
$\mathbf{q}$	displacement vector
R	shaft radius, system modal norm
S_B	bearing Sommerfeld number
t	time
$\mathbf{x}^*$	state space vector defined by equation (9)
x,y	displacements
W	bearing load
Ω	rotor speed, rad/sec
λ	eigenvalue
ϕ	right eigenvector
φ	left eigenvector
δ	logarithmic decrement
σ	damping exponent
ω	natural whirl frequency
μ	lubricant viscosity

INTRODUCTION

The design of rotor bearing systems are becoming more complex due to the increase in the rotor rotational speeds, requirements for the energy consideration, and extreme operating conditions. Typical design requirements for modern compressors include the capability of operating in the unload condition, near surge condition, a wide range of oil temperatures, and possible rotor overspeed. Very often, the instabilities caused by fluid film bearings, seals, and aerodynamic forces are the only restrictions to the wide range of operating conditions. A very large and unstable vibration

component, typically ranging from 20% to 80% of the rotor speed, can be observed by dynamic signal analyzers or FFT emulators if the system is operated beyond the instability threshold or the stability boundaries. This excessive vibration usually results in machine damage. Therefore, the determination of the instability threshold and the stability boundaries of the operating parameters is critical for the machine's safe operation.

When a rotor is operated beyond a certain rotational speed, a very high and unstable vibration component with a fractional frequency of the rotor speed will be developed. This rotor speed is referred to as the instability threshold. At a constant rotational speed, the rotor can experience the same unstable state when an operating parameter is beyond a certain value. This limit is referred to as the stability boundary of that operating parameter. The instability threshold and stability boundary are usually determined from a stability map. A map of logarithmic decrements or damping coefficients versus the operating parameter is generated by repeated calculation of eigenvalues for a range of an operating parameter under study. Lund (1974) utilized the transfer matrix method for the calculation of damped critical speeds and instability threshold by repeatedly solving the eigenvalue polynomial equation. Since then, various roots searching techniques based on the transfer matrix polynomial method were proposed by Murphy and Vance (1983), Kim and David (1990). The instability threshold is then determined graphically by a stability map. A direct numerical procedure for the determination of instability threshold based on the transfer matrix method was presented by Zhou and Rieger (1985). A quadratic interpolation and iteration schemes were used in their algorithm to determine the instability threshold and the corresponding whirl frequency. No stability boundaries on the operating parameters were discussed. The numerical difficulties involved with the transfer matrix method as the model size increases are well known. The possibility of missing some vibration modes still remains. A closed form solution of the stability parameter for a rigid and symmetric rotor system supported by two identical fluid film bearings was presented by Lund and Thomsen (1978). Rao (1983) extended the work to a flexible and symmetric rotor supported by two identical bearings. However, for the practical applications, a stability analysis of the complete rotor-bearing-foundation systems is required to determine the system stability.

The development of finite element formulations for use in the rotor-bearing-foundation systems has received considerable attention within the past few years (Nelson and McVaugh, 1976; Rouch and Kao, 1979; Nelson, 1980). The capability of modeling complex systems and the stability of the numerical algorithms make the finite element method a popular and indispensable tool in the field of rotordynamics. The effects of rotatory inertia, gyroscopic moments, shear deformation, axial loads, flexible disks and housing are included in the work. The linearized bearing and seal coefficients, aerodynamic cross-couplings, and other sources of interaction can be easily incorporated into the mathematical model. Rajan et al. (1986) presented a direct numerical algorithm for the calculation of damped critical speeds using eigenvalue sensitivity based on the finite element formulation. The parameter sensitivity in the dynamics of rotor systems was discussed in their paper. These sensitivity coefficients are valid and can be used only for a small design change. The instability threshold still has to be determined by the graphical method. Very often, the effects of the operating parameters on the system stability are essential in the design stage. The rotor speed dictates the aerodynamic performance. The lubricant viscosity determines the oil type and operating temperature range. The bearing loads determine the range of throttling. Therefore, it is extremely useful to have an automated procedure to directly calculate the instability threshold and the stability boundaries of the operating parameters.

A direct numerical procedure proposed in this paper allows the designers to determine the instability threshold and stability boundaries of the operating parameters if the boundaries exist. The governing system equations of motion are derived from the finite element method. The solution procedure is based on optimization techniques. The optimization techniques are very effective and suitable for this type of algorithm. The operating parameters are subject to constraints as dictated by practical limitations. Examples are presented to illustrate the procedure.

GOVERNING EQUATIONS OF MOTION

The finite element formulation of the rotor assembly is well documented by Nelson (1980) and Ehrich (1992). The equations of motion for the rotating assembly and foundation are of the form

$$\begin{bmatrix} \mathbf{M}_r & 0 & 0 \\ 0 & \mathbf{M}_d & 0 \\ 0 & 0 & \mathbf{M}_f \end{bmatrix} \begin{Bmatrix} \ddot{\mathbf{q}}_r \\ \ddot{\mathbf{q}}_d \\ \ddot{\mathbf{q}}_f \end{Bmatrix} + \begin{bmatrix} \mathbf{G}_r & 0 & 0 \\ 0 & \mathbf{G}_d & 0 \\ 0 & 0 & 0 \end{bmatrix} \begin{Bmatrix} \dot{\mathbf{q}}_r \\ \dot{\mathbf{q}}_d \\ \dot{\mathbf{q}}_f \end{Bmatrix} + \begin{bmatrix} \mathbf{K}_{rr} & \mathbf{K}_{rd} & \mathbf{K}_{rf} \\ \mathbf{K}_{dr} & \mathbf{K}_{dd} & 0 \\ \mathbf{K}_{fr} & 0 & \mathbf{K}_{ff} \end{bmatrix} \begin{Bmatrix} \mathbf{q}_r \\ \mathbf{q}_d \\ \mathbf{q}_f \end{Bmatrix} = \begin{Bmatrix} \mathbf{Q}_r \\ \mathbf{Q}_d \\ \mathbf{Q}_f \end{Bmatrix} \quad (1)$$

where the vectors $\mathbf{q}_r$, $\mathbf{q}_d$, $\mathbf{q}_f$ represent the displacements of shaft elements (and rigid disks), flexible disks, and flexible foundation, respectively. The mass/inertia matrix $\mathbf{M}$ is a real symmetric matrix which is a function of structural properties. The gyroscopic matrix $\mathbf{G}$ is a real skew symmetric matrix which is a function of structural properties and the shaft rotational speed, and the stiffness matrix $\mathbf{K}$ can be an arbitrary real matrix due to the nonconservative axial loads. The motion of the rotor is described by two translational and two rotational coordinate displacements at each finite element station. The motions of the flexible disks and foundation can be described by six degrees of freedom at each finite element station. The matrices of flexible disks and foundation can be obtained from any existing structural finite element computer programs, such as NASTRAN and ANSYS. The three primary structural components (shaft and rigid disks, flexible disks, and foundation) are coupled by the interconnecting components.

Fluid film bearings are commonly used in the rotating machinery due to the bearing damping, stiffness characteristics and long life of operation. The use of linearized bearing dynamic coefficients in the analysis of rotor dynamics has been

widely accepted (Lund and Thomsen, 1978; Lund, 1990). The linearized governing equation of motion for a fluid film bearing connecting shaft station i and foundation j (or station j of another shaft) is given by

$$\begin{bmatrix} \mathbf{C}_b & -\mathbf{C}_b \\ -\mathbf{C}_b & \mathbf{C}_b \end{bmatrix}\begin{Bmatrix} \dot{\mathbf{q}}_i \\ \dot{\mathbf{q}}_j \end{Bmatrix}+\begin{bmatrix} \mathbf{K}_b & -\mathbf{K}_b \\ -\mathbf{K}_b & \mathbf{K}_b \end{bmatrix}\begin{Bmatrix} \mathbf{q}_i \\ \mathbf{q}_j \end{Bmatrix}=\begin{Bmatrix} \mathbf{Q}_i \\ \mathbf{Q}_j \end{Bmatrix} \quad (2)$$

where the 2x2 matrices $\mathbf{C}_b$ and $\mathbf{K}_b$ are the bearing damping and stiffness coefficients which are determined by solving the Reynolds equation and its perturbed equations (Klit and Lund, 1986). To study the effects of bearing parameters on the system stability, the bearing dynamic coefficients are expressed in the non-dimensional formats and represented as functions of the Sommerfeld number. The bearing Sommerfeld number is defined by

$$S_B = \frac{\mu N_s}{\left(W/LD\right)}\left(\frac{R}{C_B}\right)^2 \quad (3)$$

and the non-dimensional stiffness and damping coefficients are

$$\hat{K}_{i,j}=\frac{K_{i,j}C_B}{W}\ ;\ \hat{C}_{i,j}=\frac{C_{i,j}\Omega C_B}{W} \qquad (i=x,y;j=x,y) \quad (4)$$

The Sommerfeld number and non-dimensional coefficients are sometimes normalized with respect to the lobe radial clearance. However, the bearing radial clearance is more often used in the bearing and equipment manufacturers for the measurability and machinability. Hence, the bearing radial clearance is employed in this paper. The relationship between the bearing and lobe radial clearance is related by the bearing preload:

$$m = 1 - \frac{C_B}{C_L} \quad (5)$$

For a given operating condition, a Sommerfeld number is determined and the calculation of corresponding bearing stiffness and damping coefficients becomes straightforward. Thus, for a given type of bearing, the dimensional bearing coefficients in equation (2) are functions of rotor speed, oil viscosity, bearing load, and bearing clearance.

Other sources of self-excitation include the aerodynamic effects of impellers and seals. This type of de-stabilizing forces can be expressed in the form (Weiser and Nordmann, 1989)

$$\begin{bmatrix} C_a & c_a \\ -c_a & C_a \end{bmatrix}\begin{Bmatrix} \dot{x} \\ \dot{y} \end{Bmatrix}+\begin{bmatrix} K_a & k_a \\ -k_a & K_a \end{bmatrix}\begin{Bmatrix} x \\ y \end{Bmatrix}=\begin{Bmatrix} F_x \\ F_y \end{Bmatrix} \quad (6)$$

where C_a, c_a and K_a, k_a are also functions of operating parameters.

The assembled equations of motion which describe the dynamic characteristics of the system are of the form

$$\mathbf{M}\ddot{\mathbf{q}}+[\mathbf{G}+\mathbf{C}_p]\dot{\mathbf{q}}+[\mathbf{K}+\mathbf{K}_p]\mathbf{q}=\mathbf{Q} \quad (7)$$

where $\mathbf{p}$ is the vector of the operating parameters which include rotor rotational speed, lubricant viscosity, bearing loads, bearing clearance, and axial loads, etc. The matrices $\mathbf{C}_p$ and $\mathbf{K}_p$ are quite sparse and can be rearranged for minimum storage requirement.

SYSTEM STABILITY

For a given operating condition, the stability of the dynamic system can be determined by the eigenvalue equation of the homogeneous state space form

$$\mathbf{M}^*\dot{\mathbf{x}}(t)+\mathbf{K}^*\mathbf{x}(t)=\mathbf{0} \quad (8)$$

where

$$\mathbf{M}^* = \begin{bmatrix} \mathbf{M} & \mathbf{0} \\ \mathbf{0} & \mathbf{I} \end{bmatrix}\ ;\quad \mathbf{K}^* = \begin{bmatrix} \mathbf{G}+\mathbf{C}_p & \mathbf{K}+\mathbf{K}_p \\ -\mathbf{I} & \mathbf{0} \end{bmatrix}$$

and

$$\mathbf{x}(t) = \begin{Bmatrix} \dot{\mathbf{q}}(t) \\ \mathbf{q}(t) \end{Bmatrix} \quad (9)$$

The solution has the form

$$\mathbf{x}(t) = \phi\, e^{\lambda t} \quad (10)$$

The associated eigenvalue problem becomes

$$(\lambda\mathbf{M}^* + \mathbf{K}^*)\phi = \mathbf{0} \quad (11)$$

with 2n eigenvalues λ_i and the associated eigenvectors ϕ_i.

Since $\mathbf{M}$ is a positive definite real symmetric matrix, equation (11) can be reduced to the form

$$\mathbf{A}\phi = \lambda\phi \quad (12)$$

and

$$\mathbf{A} = -(\mathbf{M}^*)^{-1}\mathbf{K}^* = \begin{bmatrix} -\mathbf{M}^{-1}(\mathbf{G}+\mathbf{C}_p) & -\mathbf{M}^{-1}(\mathbf{K}+\mathbf{K}_p) \\ \mathbf{I} & \mathbf{0} \end{bmatrix} \quad (13)$$

is an arbitrary real matrix. The solution of the eigenvalue problem is complex:

$$\lambda_i = \sigma_i + j\omega_i \qquad (i = 1,2,\ldots 2n) \quad (14)$$

The stability boundary can be established by examining the variation in the real part of λ_i as a function of an operating parameter. It is very common that logarithmic decrement is used to express the degree of the stability instead of using the damping exponent:

$$\delta = \frac{-2\pi\sigma}{\omega} \quad (15)$$

When logarithmic decrement becomes negative or the damping exponent becomes positive, the system becomes unstable and the linear theory is no longer valid. Nonlinear theory should be applied when the system operating parameter exceeds the stability boundary. However, experience shows that in most practical applications, the unstable vibration component grows very rapidly and violently such that the machine cannot be continuously operated without damage in one form or another.

NUMERICAL ALGORITHM

At the threshold of instability, the σ is zero such that

$$\lambda_{threshold} = j\omega_{threshold} \tag{16}$$

To determine the stability boundary of an operating parameter, the problem can be stated as one of choosing an operating parameter subject to practical limitation of the design such that one of the system eigenvalues has a zero real part. The corresponding imaginary part is referred to as unstable whirl frequency. In most applications, if the system becomes unstable, the rotor whirls in its first mode (lowest whirl frequency) with forward precession. It should be noted that the first unstable mode can be either a bending mode or a rigid body mode, depending upon the potential energy distribution.

The numerical algorithm can be written mathematically as follows: To find an operating parameter, p, which

$$\text{minimizes} \quad f(p) = |\sigma| \quad \text{or} \quad \sigma^2 \tag{17}$$

$$\text{and is subject to} \quad p^L < p < p^U \tag{18}$$

The operating parameters considered in this paper can be the rotor rotational speed, lubricant viscosity, bearing loads, bearing clearance, and axial loads, etc. The optimization procedure is terminated at the ith iteration step if the objective function, $f(p)$, satisfies the following conditions:

$$f(p) < Epsilon \tag{19}$$

or

$$|f(p)^i - f(p)^{i-1}| < Epsilon \tag{20}$$

where $Epsilon$ is a small number defined by the users. If the convergence equation (19) is satisfied, the instability boundary is then established. If the procedure stops due to convergence equation (20), no instability boundary will be established and the system is either in a stable or an unstable state throughout the limits of the operating parameter. The feasible direction method (Vanderplaats, 1984) is employed as the optimization solver. The gradients required in the iterative process can be obtained analytically in the following expression (Rajan et al., 1987)

$$\frac{\partial \lambda_i}{\partial p} = \frac{-\varphi_i^T \left(\lambda_i \frac{\partial \mathbf{M}^*}{\partial p} + \frac{\partial \mathbf{K}^*}{\partial p} \right) \phi_i}{R_i} \tag{21}$$

where ϕ_i, φ_i are the corresponding right and left eigenvectors, respectively. The right eigenvector is defined in equation (12) and the left eigenvector is defined in the following equation

$$\varphi^T \mathbf{A} = \lambda \varphi^T \tag{22}$$

The associated modal norm is defined as

$$R_i = \varphi_i^T \mathbf{A} \phi_i \tag{23}$$

The matrices in equation (23) are quite sparse. Computational procedures may be adopted which allow for the calculation of eigenvalue sensitivities with minimum computational expense (Rajan et al., 1987). To determine the instability boundary, only the real part of equation (21) is used.

PARAMETRIC STUDIES

A single journal bearing system (Kirk and Gunter, 1970) is used for the parametric studies. The physical parameters of the system are summarized in Table 1

Journal Mass = 22.766 Kg (0.13 Lbf-sec^2/in)
Bearing Length = 12.7 mm (0.5 in)
Bearing Diameter = 50.8 mm (2.0 in)
Bearing Clearance = 0.0635 mm (0.0025 in)
Bearing Load = 222.4 N (50 Lbf)
Oil Viscosity = 6.89478 Centipoise (1.0E-06 Reyns)

Table I System Parameters

For a single journal bearing system, the rotor is assumed to be rigid and symmetric which is usually not practical. The stability of a rotor-bearing system depends on the bearing characteristics, bearing locations, rotor stiffness, and operating speed, etc. Therefore, for a given rotating system it is necessary to determine the stability boundaries by using a complete system model including rotor, bearing properties, and all other effects. This simple two degrees of freedom system is only employed to demonstrate the validity of the numerical procedures proposed in this paper. The results obtained from the algorithm presented here can be easily verified by using the conventional graphical method.

Using the analytical procedures described earlier, the instability threshold can be found to be around 14025 rpm by considering the rotational speed as the operating parameter. For the purpose of comparison, the whirl speed and stability maps shown in Figures 1 and 2 are generated by calculating system eigenvalues over a range of rotational speed. Figure 1 shows that the backward mode is a real non-vibratory mode with zero whirl frequency from zero to 4615 rpm and becomes a vibratory mode after 4615 rpm. The forward mode is always a vibratory mode throughout the speed range. Figure 2 shows that the forward mode becomes unstable as the speed exceeds 14025 rpm. The instability threshold determined by using the proposed procedure is in good agreement with the result obtained from the stability map. A parametric study is then carried out to understand the influence of the individual parameter on the instability threshold. Figure 3 shows that the instability threshold decreases as the oil viscosity increases and it is very sensitive at the low viscosity range (i.e. high temperature range). Figure 4 shows that decreasing the bearing load monotonously lowers the instability threshold. Figure 5 shows that the lowest instability threshold occurs when the bearing clearance is around 0.0575 mm and the system stability can be improved by either decreasing or increasing the clearance from that point.

At 12000 rpm, the stability boundaries of the bearing load and oil viscosity were calculated to be around 185 N and 9.1 Centipoise, respectively. The logarithmic decrements versus bearing load and oil viscosity at 12000 rpm are plotted in Figures 6 and 7 for the comparison purpose. Figure 6 shows that the logarithmic decrement of the forward mode decreases as the bearing load decreases. On the contrary, the logarithmic decrement of the backward mode slightly increases as the bearing load decreases. The forward mode becomes unstable

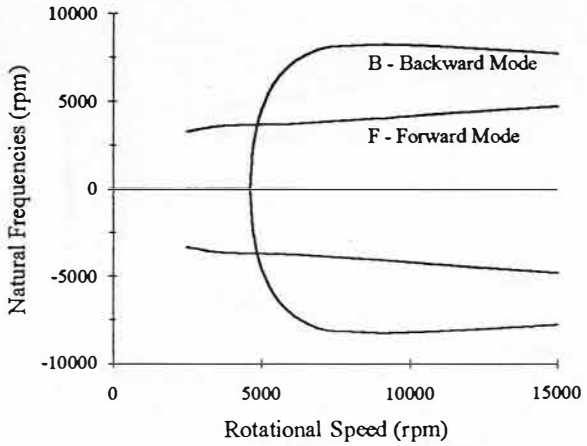

FIG. 1 WHIRL SPEED MAP

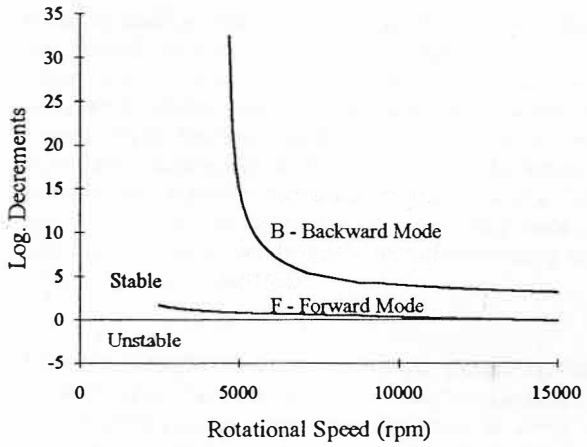

FIG. 2 STABILITY MAP

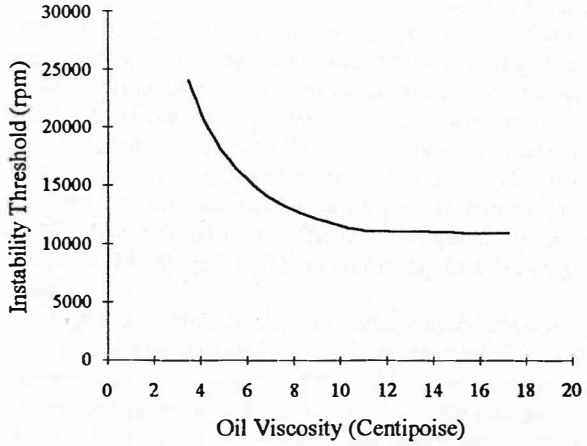

FIG. 3 INSTABILITY THRESHOLD VS. OIL VISCOSITY

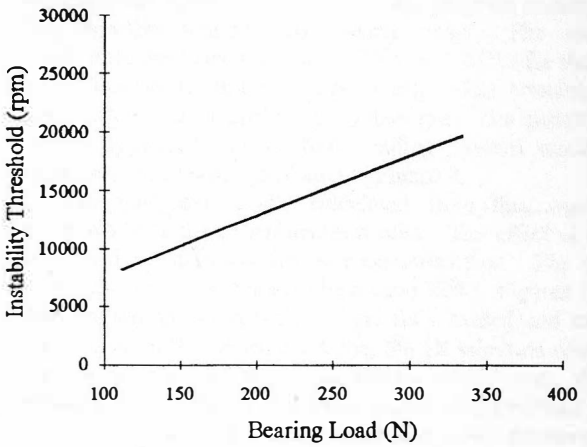

FIG. 4 INSTABILITY THRESHOLD VS. BEARING LOAD

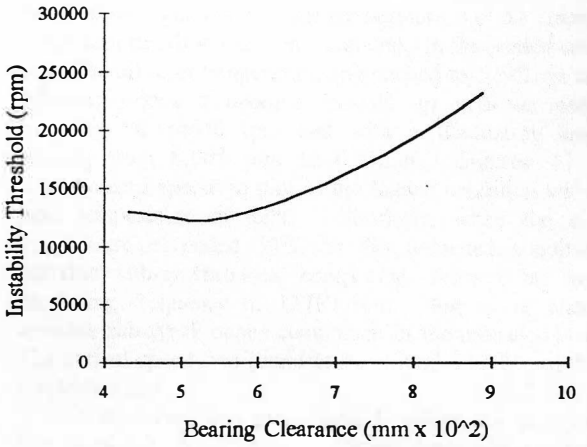

FIG. 5 INSTABILITY THRESHOLD VS. BEARING CLEARANCE

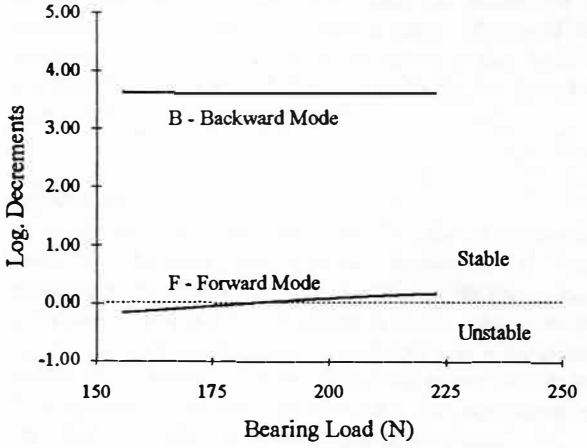

FIG. 6 LOGARITHMIC DECREMENTS VS. BEARING LOAD

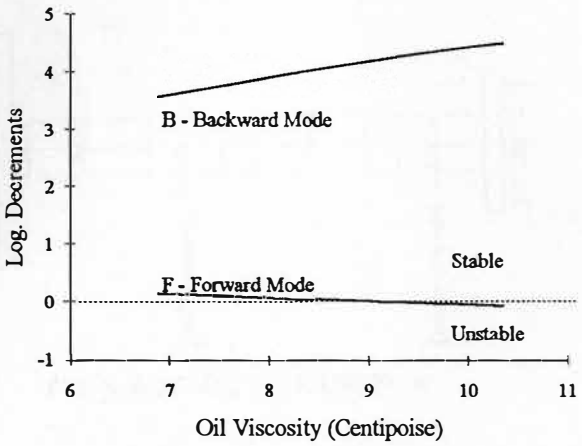

FIG. 7 LOGARITHMIC DECREMENTS VS. OIL VISCOSITY

when the bearing load is less than 185 N. Figure 7 shows that the forward mode becomes unstable when the oil viscosity is larger than 9.1 Centipoise. The logarithmic decrement of the backward mode increases and the logarithmic decrement of the forward mode decreases as the oil viscosity increases. The logarithmic decrements of the forward and backward modes move in the opposite directions as the operating parameter varies. Under normal circumstances, the forward mode becomes unstable. This effect can be mathematically proven by using the energy approach (Lund 1990).

APPLICATIONS TO AN INDUSTRIAL COMPRESSOR

To illustrate the practical application of the algorithm, a high speed centrifugal compressor was employed as a test vehicle. The single overhung rotor system has a length of 550 mm and a bearing diameter of 55 mm. The rotating assembly weighs about 17 Kg and is supported by two 3-lobe bearings as indicated in Figure 8. ISO VG 32 mineral oil was used in the test. The bearing loads are mainly due to the gear force which varies from 110 Kg to 450 Kg depending on the loading condition. The oil temperature regulating valve was disabled during the test in order to manually adjust the oil temperature. Two perpendicular vibration probes were located at station 4 between the impeller and bearing. The effects of the bearing loads and oil temperature on the stability were studied. The first three forward synchronous rigid bearing critical speeds are 17730, 80720, and 177260 rpm. The rotor is operated at a constant speed of 29700 rpm which is above the first bending critical speed.

In the analytical model, an aerodynamic cross-coupling of 350 N/mm was included in the finite element station 2. The cross-coupling was calculated from the Alford equation with the correlation factor of 1.5 (Kirk, 1988). In the calculation of the bearing load instability boundary, the convergence equation (20) was met and the program stopped. Hence no instability boundary was established and the system is in a stable state throughout the limits of bearing load. In the calculation of the oil temperature instability boundary, the program converged and the objective function was nearly zero. The instability boundaries were calculated to be 59°C and 61°C for the loaded and unloaded conditions, respectively. The unstable whirl frequency was calculated around 15000 rpm. The unstable mode in this application is the first bending forward mode. The associated mode shape is plotted in Figure 9.

The analytical results calculated from this work were compared with the experimental results. The effect of bearing load on the system stability was examined first. The oil inlet temperature was controlled to be around 38°C. Figures 10A and 10B are the spectrum plots for the fully loaded and unloaded conditions. In the loaded condition, the 1X vibration component was steady with an amplitude around 0.0075 mm, the sub-synchronous and higher harmonics were relatively small. In the unloaded condition, the 1X vibration component fluctuated from 0.008 mm to 0.011 mm and the sub-synchronous and higher harmonics were relatively small. The sub-synchronous component occurred around 16500 rpm. The system was in a stable operation for any loading conditions at 38°C inlet oil temperature. The effect of oil temperature, i.e. oil viscosity, on the system stability was then examined. In the loaded condition, when the oil inlet temperature approached to 52°C, an unstable sub-synchronous component showed up with an oscillating frequency of 14640 rpm and with a fluctuating amplitude ranging from 0.008 mm to 0.02mm. Figures 11 is the instantaneous spectrum plot in the loaded condition with an oil inlet temperature of 52°C. Similarly, when the oil inlet temperature exceeded 50°C in the unloaded condition, the unstable sub-synchronous component showed up with an oscillating frequency of 14760 rpm. Figure 12 shows the unstable sub-synchronous component in the unloaded condition. The critical speed was found to be around 14600 rpm from the coastdown plot.

The analytical and experimental results are in agreement. The instability boundaries of the oil temperature established analytically were slightly higher than the values obtained from the experiment. The difference can be attributed to the measurement of the oil inlet temperature, the assumption made in the hear balance calculation, and the estimation of the aerodynamic cross-coupling. This example illustrated that the proposed algorithm can be an effective design tool in the establishment of the instability boundaries of the operating parameters.

CONCLUSION

A direct numerical algorithm for the determination of instability threshold and stability boundaries of operating parameters for the flexible rotor-bearing systems has been presented. The onset of instability is established by examining the variation in the real part of eigenvalue as a function of an operating parameter. The automated algorithm can be used for improvement of system stability and for adjustment of the operating parameters to a wide range of operation.

Two examples have been presented to demonstrate the automated algorithm. A parametric study on the instability threshold was carried out in the first example to show the

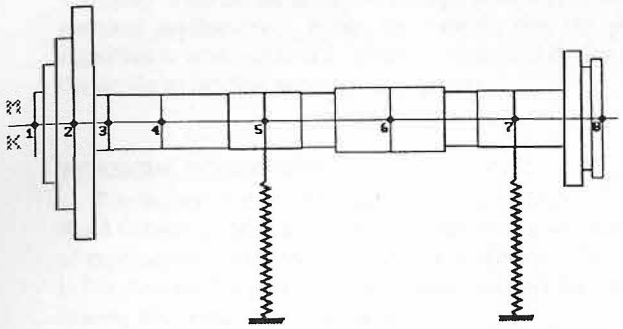

FIG. 8 ROTOR CONFIGURATION

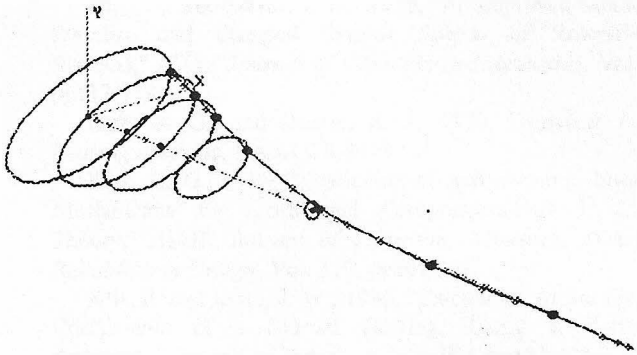

FIG. 9 UNSTABLE FORWARD PRECESSION MODE

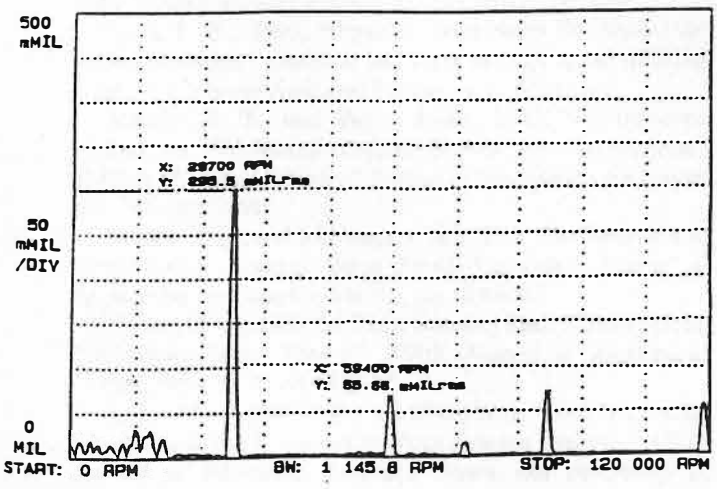

FIG. 10A TEST RESULTS AT 38°C LOADED CONDITION

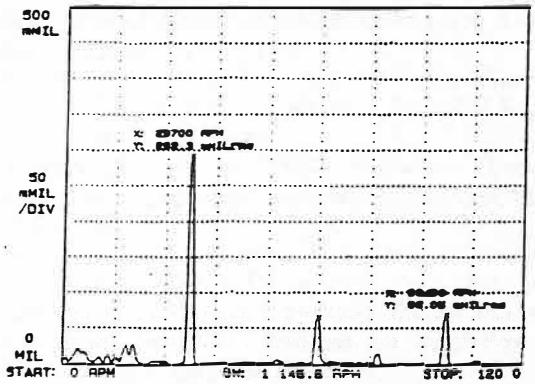

FIG. 10B TEST RESULTS AT 38°C LOADED CONDITION

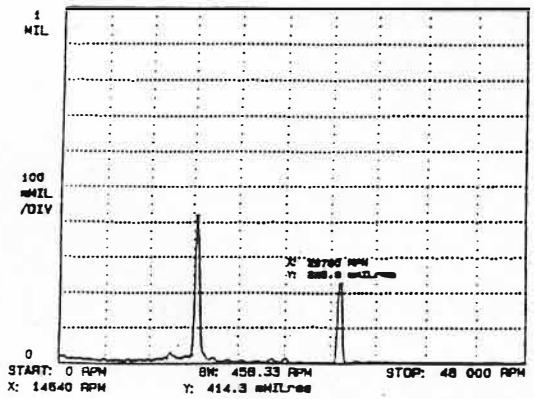

FIG. 11 TEST RESULTS AT 52°C LOADED CONDITION

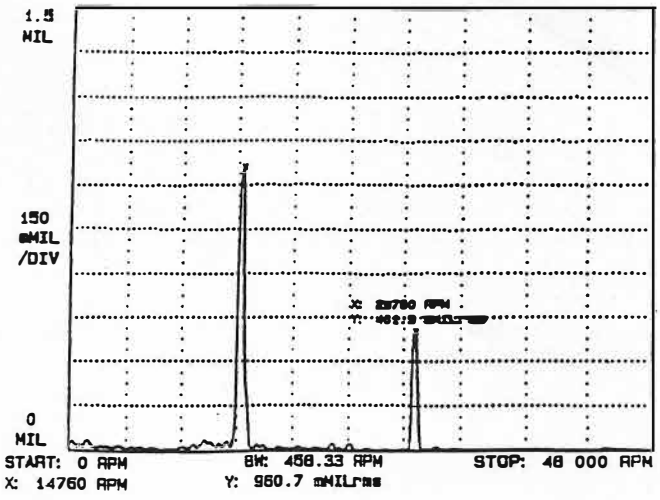

FIG. 12 TEST RESULTS AT 50°C UNLOADED CONDITION

influence of the operating parameters on the system stability. An industrial high speed compressor has been employed as a test vehicle to illustrate the ability of the algorithm to deal with more practical applications. It has been shown that the proposed algorithm is a valuable and effective analytical design tool for the design of flexible rotor bearing systems.

ACKNOWLEDGMENTS

The author wishes to thank Mr. Filippo Mariani, Ingersoll-Rand Company, Italy, for his contribution to the implementation of experimental work on the industrial compressor. Thanks also to Ms. Loretta Rodgers and Ms. Allyson Benefiel for their proof reading and word processing work.

REFERENCES

Ehrich, F. F., 1992, *Handbook of Rotor-dynamics*, McGraw-Hill, New York, Chapter 2.

Kim, D., and David, J. W., 1990, "An Improved Method for Stability and Damped Critical Speeds of Rotor-Bearing Systems," *ASME Journal of Vibration and Acoustics*, Vol. 112, ppl 12-118.

Kirk, R. G., and Gunter, E. J., 1970, *Transient Journal Bearing Analysis*, NASA CR-1549.

Kirk, R. G., 1988, "Evaluation of Aero-dynamic Instability Mechanisms for Centrifugal Compressors-Part 1: Current Theory," *ASME Journal of Vibration, Acoustics, Stress and Reliability in Design*, Vol. 110, pp201-206.

Klit, P. and Lund, J. W., 1986, "Calculation of the Dynamic Coefficients of a Journal Bearing, Using a Variational Approach," *Journal of Tribology*, Vol. 108, pp421-425.

Lund , J. W., 1974, "Stability and Damped Critical Speeds of a Flexible Rotor in Fluid-Film Bearings," *ASME Journal of Engineering for Industry*, Vol. 96, No. 2, pp. 509-517.

Lund, J. W., and Thomsen, K. K., 1978, "A Calculation Method and Data for the Dynamic Coefficients of Oil-Lubricated Journal Bearings," *ASME Topics in Fluid Film Bearing and Rotor Bearing System Design and Optimization*, pp. 1-28.

Lund, J. W., 1990, "Dynamic Coefficients for Fluid Film Journal Bearings," *Vibration and Wear in High Speed Rotating Machinery*, Kluwer Academic Publishers, pp605-616.

Murphy, B. T., and Vance, J. M., 1983, "An Improved Method for Calculating Critical Speeds and Rotordynamic Stability of Turbomachinery," *Journal of Engineering for Power*, Vol. 105, pp591-595.

Nelson, H. D., and McVaugh, J. M., 1976, "The Dynamics of Rotor-Bearing Systems Using Finite Elements," *Journal of Engineering for Industry*, Vol. 98, pp. 593-600.

Nelson, H. D., 1980, "A Finite Rotating Shaft Element Using Timoshenko Beam Theory," *ASME Journal of Mechanical Design*, Paper no. 79-WA/DE-5.

Rajan, M., Nelson, H. D., and Chen, W. J., 1986, "Parameter Sensitivity in the Dynamics of Rotor-Bearing Systems," *ASME Journal of Vibration, Acoustics, Stress and Reliability in Design*, Vol. 108, pp197-206.

Rao, J. S., 1983, "Instability of Rotors in Fluid Film Bearings," *ASME Journal of Vibration, Acoustics, Stress and Reliability in Design*, pp274-279.

Rouch, K. E., and Kao, J. S., 1979, "A Tapered Beam Finite Element for Rotor Dynamics Analysis," *Journal of Sound and Vibration*, Vol. 66, pp119-140.

Vanderplaats, G. N., 1984, *Numerical Optimization Techniques for Engineering Design with Applications*, McGraw-Hill, New York.

Weiser, H. P. and Nordmann R., 1989, "Calculation of Rotordynamic Coefficients for Labyrinth Seals Using a Three Dimensional Finite Difference Method," *The 6th Workshop on Rotordynamic Instability Problems in High-Performance Turbomachinery*, Texas A&M University.

Zhou, S. and Rieger, N. F., 1985, "An Instability Analysis Procedure for Three-Level Multi-Bearing Rotor-Foundation Systems," *Symposium on Instability in Rotating machinery*, Carson City, Nevada.